

Performance analysis of super capacitor integrated PV fed multistage converter with SMC controlled VSI for varying nonlinear load conditions

Shruti Pandey^{1*}, Bharti Dwivedi¹, Anurag Tripathi¹

¹ Department of Electrical Engineering, Institute of Engineering and Technology, Lucknow, India

*Corresponding author E-mail: shruti.eeee@gmail.com

Abstract

This work comprises of an MPPT (maximum power point tracking) controlled Photovoltaic (PV) source, in combination with a supercapacitor, cascaded with a Sliding Mode Controlled (SMC) Inverter, which supplies varying nonlinear loads. The varying solar irradiation effects and its intermittency have been successfully managed by the boost converter controlled by MPPT and supercapacitor controlled by bidirectional converter. The bidirectional converter step down and step up the terminal voltage and provides the power flow in a bidirectional manner. The proposed model helps in obtaining the seamless action under changing irradiation and for varying load conditions. The performance of the SMC controlled Inverter, when compared with a PI controlled Inverter, has been found to be superior in terms of power quality and robustness of the supply system.

Keywords: Photo Voltaic; Bidirectional Converter; DC-DC Boost Converter; Maximum Power Point Tracking; Sliding Mode Control; Supercapacitor; Voltage Source Inverter.

1. Introduction

The solar energy source is the most accepted energy source among all the accessible renewable energy sources for all power applications. In solar fed microgrid system, inverters play a very important role at the load end for different applications.

In order to provide good quality stable output in terms of output voltage and THD or in terms of transient performance like quick settlement against load and source variations, advanced strategies of control are desired to be used with Voltage source Inverters [1]. There are numerous control strategies for voltage source inverter (VSI). Traditionally used PI control, is not capable of tracking periodic signals accurately, whereas the basic hysteresis current control that generates a variable switching frequency requires the use of suitable filter with it. Multiple feedback loop control method with temperate switching frequency makes output voltage waveform purely sinusoidal [2] however; in case of non-linear loads it gives imprecise output voltage. H infinity robust state feedback control undergoes realization difficulty as it is higher order.

All the above linear controllers performs satisfactorily around equilibrium point only, but for guarantying the overall stability of the VSI system under large perturbations the non-linear controllers performs better. One of the widely used non-linear controllers is Passivity-Based Control (PBC) [6, 7]. However in PBC method, the global asymptotic stability is assured with the perfect parameter match supposition which is not suitable in practice and therefore steady-state error is there in the output voltage. Sliding Mode Control (SMC) is one of the non-linear control method which is better in terms of stability, ease, regulation and robustness under broad range of operating conditions [12]. The main benefit of SMC's performance against any variation or uncertainty in the

system parameters or in the loads [13–14] is its high-speed tracking capability and superior stabilization which is helpful in mounting high-performance of VSI circuits. [15], [16], [17]

The supercapacitor (or ultracapacitor) has acquired a wide attention as balancing source of power to PV systems due to its high power density (kW/kg), longer life, large charge and discharge-cycles, lower equivalent series resistance, lesser heating losses and broader temperature range in comparison to that of batteries [18], [19]. The use of a Bidirectional dc-dc converter helps in allowing charging and discharging currents to flow to and from the supercapacitor as per the requirement.

2. Methodology

This work comprises of a PV fed multistage system where varying non-linear (Bridge rectifier) loads are considered. In the first stage the maximum power is extracted from PV system and the output of PV is boosted. A varying solar irradiation is introduced in the system and the Boost converter helps in increasing the output of PV Panel. A supercapacitor has been incorporated to balance the PV power generation, it supplies power when there is decrease in PV power generation. In the second stage controlled inverter is used for obtaining good quality ac power. Two controllers i.e. PI controller and SMC controller are individually used to control inverter in order to compare their individual performance on VSI. Further the value of filter inductor and filter capacitor is reduced to 20% of their actual value and the performance of controlled VSI is then analysed. Nonlinear loads are considered at the load end as most of the practical loads are nonlinear in nature.

2.1. Proposed system configuration

The block diagram of proposed system is shown in Figure 1. The block diagram consists of a PV Panel with variable input irradiation, its output is given to DC-DC boost converter, and for tracking maximum power MPPT algorithm is used. Super capacitor along with charge controller is used to interface with Dc link at the input of the inverter. Further controlled VSI is used to convert DC link power into ac power for feeding the non linear loads.

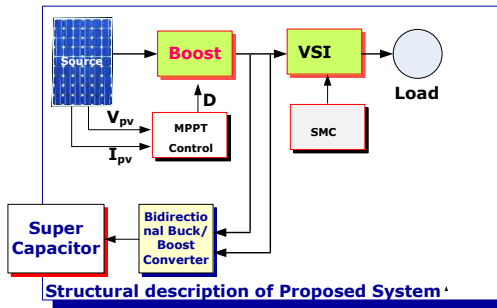


Fig. 1: Block Diagram of Proposed Configuration.

Figure 2 shows a single phase VSI with RL load. The output of the Inverter is given by V_0 and U is the control variable of the VSI.

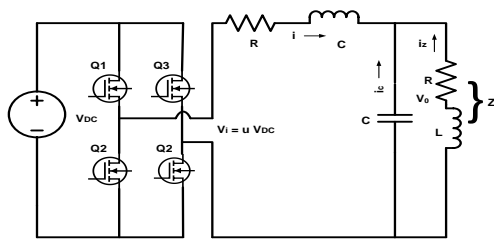


Fig. 2: Inverter.

The state space model of the inverter based on the state variables, given below, is used in the sliding surface in Sliding Mode Controller. Here V_0 and i are the state variables.

$$\dot{x} = F x + H u$$

$$F = \begin{bmatrix} -\frac{1}{ZC} & \frac{1}{C} \\ -\frac{1}{L} & 0 \end{bmatrix}$$

$$H = \begin{bmatrix} 0 \\ \frac{V_{DC}}{L} \end{bmatrix}$$

The output equation with V_0 as output can be written as

$$C = [1 \ 0]$$

3. Controllers used

3.1. MPPT control

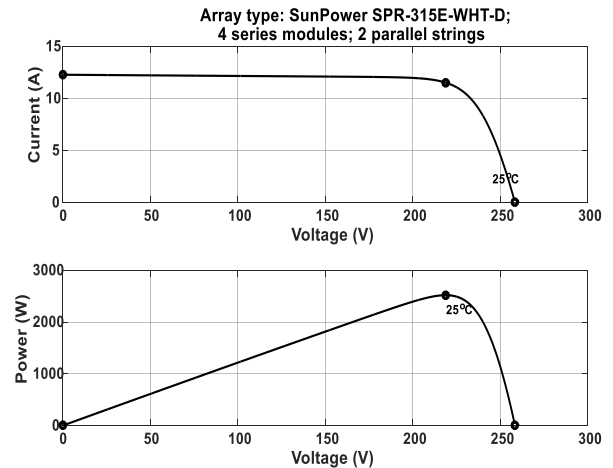


Fig. 3: I-V and P-V Characteristics at 1000 W/M2 and 25 °C.

Fixed type P and O MPPT is used here to make it easily implementable. The P-V and I-V characteristics of the PV panel is shown in Fig3.

3.2. Supercapacitor charge management control

Charging and discharging of supercapacitor is performed in two steps shown in Figure 4 and Figure 5[20]

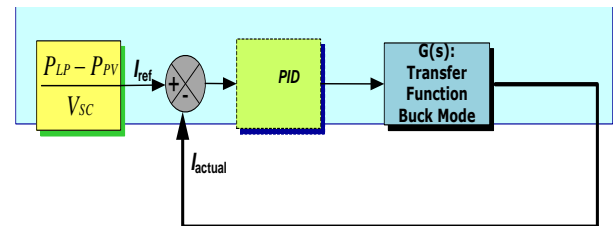


Fig. 4: Constant Current Charging Method.

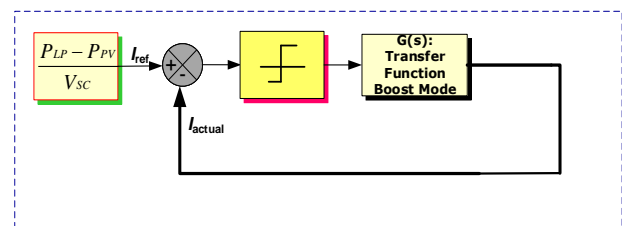


Fig. 5: Constant Current Discharging Method.

3.3. Proposed sliding mode control

Multi loop controllers are known to give better results when overall system stability and transient performance is considered, therefore in this system inner loop control, i.e. current loop control is also considered .In the SMC used in the paper, the current error is generated from voltage error and is used as inner loop control. This controller operates at very high switching frequency such that the capacitor output voltage V_C and the input inductor current i_L track precisely their respective reference values.

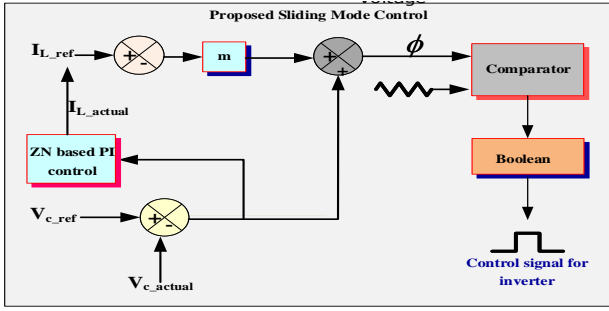


Fig. 6: Proposed Control Scheme.

Here the errors of capacitor voltage and inductor current is taken as state variables. The proposed sliding surface is a linear combination of such state variable.

$$\phi = V_{error} + mI_{error} \quad (1)$$

Where

$$V_{error} = V_{Cref} - V_C$$

$$I_{error} = i_{Lref} - i_{L1}$$

m = sliding coefficient

The controller consists of inductor current i_{L1} and output voltage V_{C2} feedback.

$$i_{Lref} = \left(k_p + \frac{k_i}{s} \right) [V_{Cref} - V_C] \quad (2)$$

Where K_p is proportional constant and K_i is integral constant of the PI controller.

When SMC controller drives the VSI towards the singular point, it makes

$$\phi = 0 \quad (3)$$

Equating $\phi = 0$ in equation (1), $0 = V_{error} + mI_{error}$

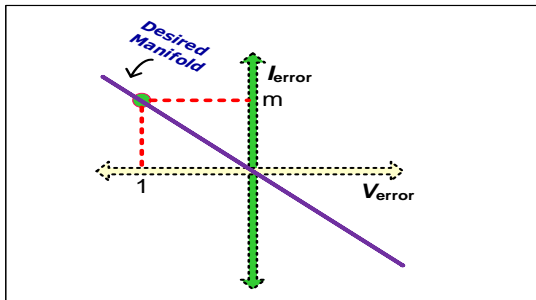


Fig. 7: Proposed Sliding Plane.

Therefore,

$$V_{error} = -mI_{error} \quad (4)$$

From closed loop model control effort can be realized as

$$u = V_{error} + mI_{error}$$

$$u = \begin{bmatrix} 1 & m \end{bmatrix} \begin{bmatrix} V_{error} \\ I_{error} \end{bmatrix} \quad (6)$$

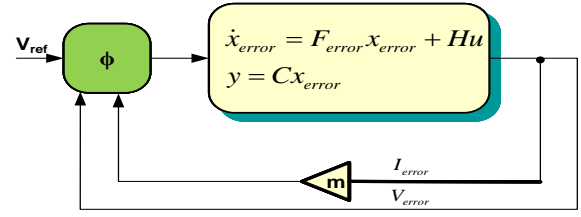


Fig. 8: Closed Loop Control Model of Proposed System.

Without loss of generality according to state feedback method

$$u = -kx_{error} \quad (7)$$

Comparing equation (6) and (7)

$$k = \begin{bmatrix} 1 & m \end{bmatrix}$$

As a result of new error state variables the state space representation of VSI system can be represented as:

$$\dot{x}_{error} = F_{error}x_{error} + Hu \quad (8)$$

$$y = Cx_{error} \quad (9)$$

The value of F_{error} is obtained as follows [12]

$$F_{error} = [I - H(kH)^{-1}u]F \quad (10)$$

From equation (10):

$$F_{error} = \begin{pmatrix} -\frac{1}{ZC} & \frac{1}{C} \\ \frac{1}{mZC} & -\frac{1}{mC} \end{pmatrix} \quad (11)$$

Keeping value of (7) in (8)

$$\dot{x}_{error} = F_{error}x_{error} + H(-kx_{error}) \quad (12)$$

$$\dot{x}_{error} = [F_{error} - Hk]x_{error} \quad (13)$$

Let F be denoted by $[F_{error} - Hk]$

The value of sliding coefficient m can be calculated in form of Eigen values as

$$[\lambda I - F] = 0 \quad (14)$$

$$\begin{pmatrix} \lambda + \frac{1}{ZC} & -\frac{1}{C} \\ \frac{1}{mZC} + \frac{V_{DC}}{L} & \lambda + \frac{1}{mC} + \frac{mV_{DC}}{LZC} \end{pmatrix} = 0 \quad (15)$$

$$\lambda^2 + \frac{\lambda}{mC} + \frac{\lambda mV_{DC}}{L} + \frac{\lambda}{ZC} + \frac{mV_{DC}}{LZC} + \frac{V_{DC}}{C} = 0 \quad (16)$$

The value of m can be obtained by comparing the above equation with the characteristics equation of desired system where

$$T_s = 1 \times 10^{-4} \text{ sec}, \xi = 0.8$$

Then from

$$T_s = \frac{3}{\xi\omega_n}$$

$$\omega_n = 3.75 \times 10^4$$

Then from standard second order system characteristics equation

$$s^2 + 2\xi\omega_n s + \omega_n^2 = 0$$

Characteristics equation of the desired system becomes

$$\lambda^2 + (6 \times 10^4)\lambda + (3.75 \times 10^4)^2 = 0 \tag{17}$$

Substituting values specified below in equation (16) and comparing with equation (17) will yield sliding mode coefficient $m = 14.7$.

The parameters of the system used for simulation results are $V_{DC} = 500V$, $Z = 528 \Omega$, $L = 1mH$, $C = 100\mu F$

Now the Eigen values obtained by

$$[\lambda I - F_{error}] = 0 \tag{18}$$

$$\begin{pmatrix} \lambda + \frac{1}{ZC} & -\frac{1}{C} \\ \frac{1}{mZC} & \lambda + \frac{1}{mC} \end{pmatrix} = 0 \tag{19}$$

$$\lambda^2 + \frac{\lambda}{mC} + \frac{\lambda}{ZC} = 0 \tag{20}$$

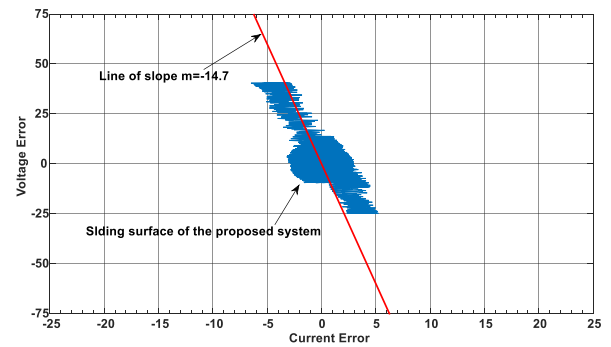


Fig. 9: Simulation Result of Sliding Plane of Proposed System.

By taking sliding coefficient as $m = 14.7$ as calculated above Eigen values of comes out to be $\lambda_1 = 0$, $\lambda_2 = -69.9$. Therefore it is clearly seen that the Eigen values obtained will always be located on the left-half of the s-plane denoting the system stability.

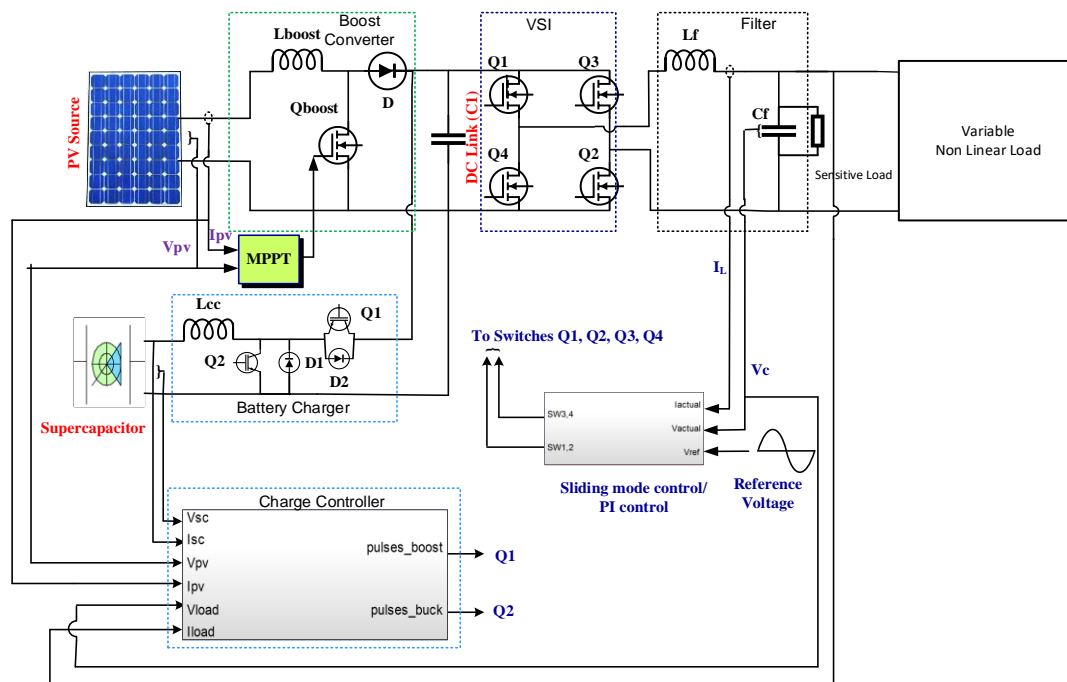


Fig. 10: Multistage Converter with SMC /PI Controlled Inverter for Nonlinear Load.

4. Results and discussion

The simulations are performed with PV panel as primary energy source giving DC voltage of 250 Volt. The PV parameters considered here for Solar Irradiation of $1000W/m^2$ are $V_{oc} = 64 \times 4 = 256V$, $I_{sc} = 6.14A$, $I_{mpp} = 5.76A$, $V_{mpp} = 54.7V$. This PV voltage is boosted up with the help of MPPT controlled boost converter which gives the output around 500Volt DC. Here solar irradiation is varied at particular intervals. The PV panel is initially given irradiation of $1000 W/m^2$. It is increased to $1200 W/m^2$ and reduced to $500 W/m^2$ at 0.5 sec and 0.85 sec respectively. This results in the variation of PV output voltage. In addition to the variation of irradiation, the load power is also varied in order to study the stability of the system in the presence of load disturbances. By connecting a parallel RL load in existing load, the load

power is raised from 2500W to 3000W and brought back to 2500W at 0.24sec and 0.35sec respectively, with this a reference power is made and actual power is compared in the upcoming waveforms. The output voltage of PV panel as seen by the DC link changes with change in irradiation, where the supercapacitor, having output of 250V, managed by its charge controller (bidirectional buck boost converter): acts to maintain a constant output voltage of 500V at the DC link.

The reference capacitor voltage is considered as $325\sin\omega t$. The load current is multiplied by 2 for the purpose of clarity. The inductor current is obtained by passing error capacitor voltage through PI Controller, whose K_p and K_i values are evaluated through Z-N based technique.

4.1. Performance analysis of PV fed multi stage convert-er with PI controlled VSI for nonlinear load

Simulation results shown in Figure 11 reveal that the irradiation based changes in PV output (Figure 11c) are effectively compli-mented by the supercapacitor Figure 11 (b) to meet the load varia-tion Figure 11 (a). The increased load power between 0. 24sec to 0.34sec as shown in Figure 11 (a) is met by supercapacitor as shown by Figure 11 (b) with the help of its charge controller (buck-boost converter). It is clear from Figure 11 (a), (b), (c) that an increase in load power in the interval of 0.24sec to 0.34 sec is exclusively met by the supercapacitor and not by the PV source. Figure 11 (d) corroborates this fact by showing a decreasing SOC in this duration. Further the irradiation is increased from 1000 W/m² to 1200 W/m² at 0.5 sec and decreased from 1200 W/m² to 500 W/m² at 0.85sec. Figure 11 (b) and Figure 11 (c), (d) shows that the supercapacitor gets charged (by buck action of buck boost converter) in the interval from 0.5sec to 0.85sec from PV panel such that a constant power of 2500 W is maintained across the load similarly from 0.85sec to 1.1sec the PV output is reduced and the supercapacitor discharges (by boost action of buck boost con-verter) to maintain a constant power supply to the load.

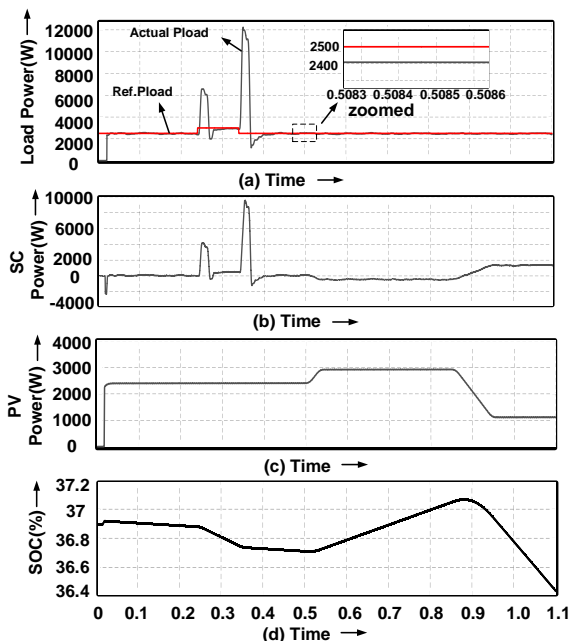


Fig. 11: Output Load Power, SC Power and PV Power for PI Controlled VSI.

The initial dip in power output of supercapacitor is attributed to the initial charging of the supercapacitor. Further the initial delay in the output power from PV array is due to the time taken by PV array to generate maximum power of 2500W. The zoomed part of load power waveform in Figure 11 (a) shows the difference between reference load power and the actual load power is 100 Watt. This difference remains throughout up to 1.1sec. There are two spikes visible at the instant of load variation in the waveform at 0.24 sec and 0.34 sec. It is due to the presence of instant charging of capacitor in the nonlinear load.

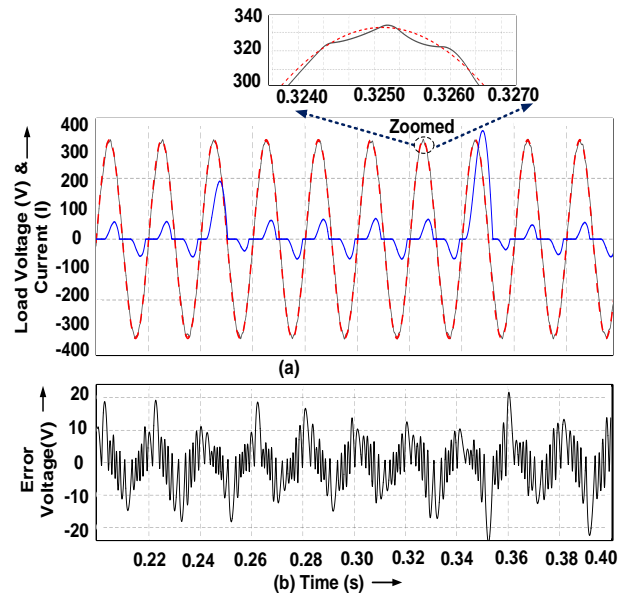


Fig. 12: PI Controlled VSI Output Voltage Waveform Showing Error = 21.54 V.

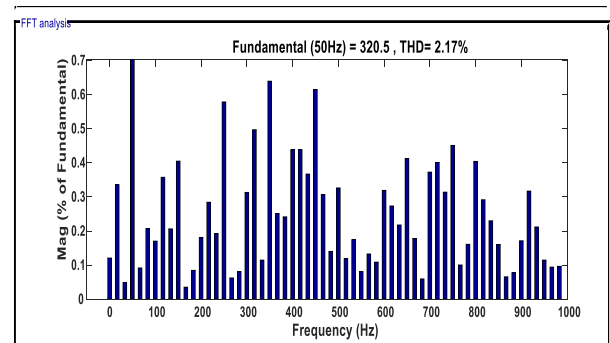


Fig. 13: THD for PI Controlled VSI Output Voltage Waveform=2.17%.

Figure 12 (a) shows the actual output capacitor voltage, reference voltage waveforms, and the current waveform, Figure 12(b) shows its error voltage waveform which has error of 21.54Volt. The THD in the output voltage of PI controlled VSI is shown in Figure 13.

4.2 Performance analysis of PV fed multi stage convert-er with SMC controlled VSI for nonlinear load

Figure 14 reveals that on changing the load the load power settles to reference power with a difference of only 4Watts in a few milli-seconds only. Figure 15 shows the tracking of voltage across cap-a-citor to its reference voltage along with the error voltage which is equal to 1.2 Volt.

The zoomed portions of Figure 12 and Figure 15 show that tracking of capacitor voltage to its reference voltage matches perfectly with Sliding Mode Controller as against the PI controller in non-linear load. Thus the performance of SMC controller is superior for nonlinear load.

Figure 16 shows that irrespective of the spikes in output current waveform, the current waveform across sensitive load is pure sinusoidal which is a good finding in terms of power quality. With this it can be concluded that whenever any critical load say hospi-tal load is connected in parallel with nonlinear load its supply is not interrupted or distorted as an effect of nonlinear load. The performance of VSI deploying SMC is depicted in Figure 17.

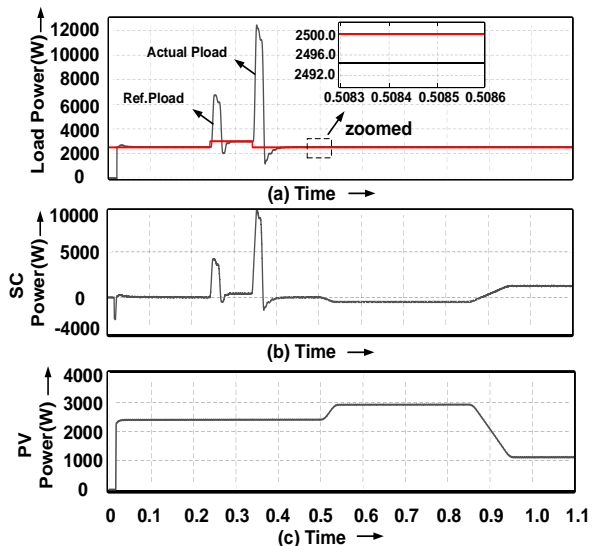


Fig. 14: Output Waveforms of Load Power, SC Power and PV Power for SMC Controlled VSI.

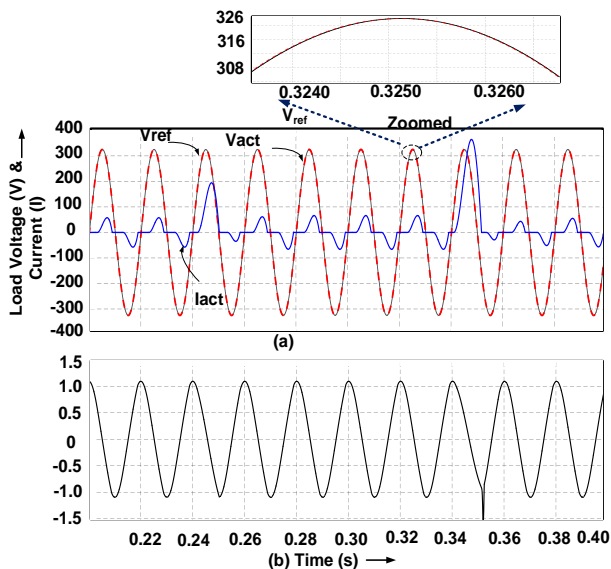


Fig. 15: SMC Controlled VSI Output Voltage Waveform Showing Error = 1.2 Volts.

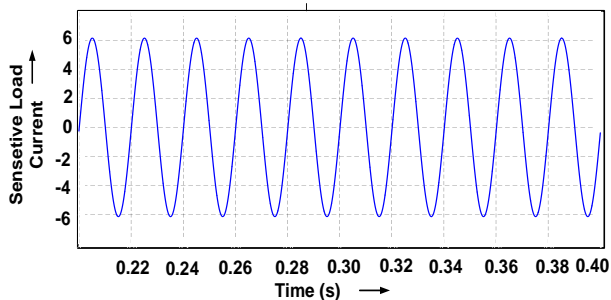


Fig. 16: Load Current Waveform of Sensitive Load.

Further to verify the robustness of Sliding mode controller over PI controller, the value of filter inductor and filter capacitor is reduced to 20% of their original value and their performance is analysed on the basis of error voltage and THD, and the results are depicted in Table 2.

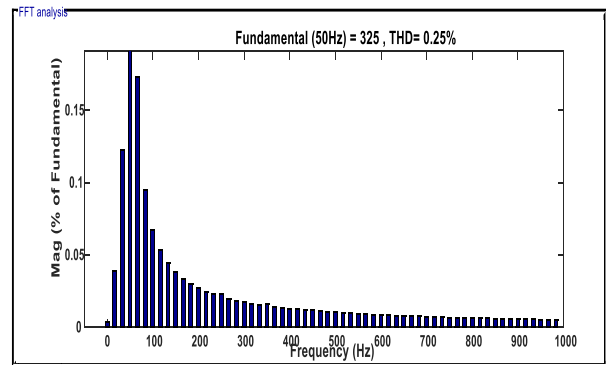


Fig. 17: THD for SMC Controlled VSI Output Voltage Waveform=0.25%.

4.3. Comprehensive analysis of findings

Table 1: Comparative Table

Type of Multi-stage System	SMC CONTROLLED VSI FOR NON LINEAR LOAD	PI CONTROLLED VSI FOR NON LINEAR LOAD
THD	0.25%	2.17%
Verr (max)	1.3 V	21.54V
Steady state error in Power	4W	100W

Table 2: Comparative Table for Change in Filter Values

Type Of Multistage System	Smc Controlled Vsi For Non Linear Load	Pi Controlled Vsi For Non Linear Load
Thd For 20% Decrease In Filter Inductor	0.27%	2.20%
Thd For 20% Decrease In Filter Capacitor	0.28%	2.23%
Thd For 20% Decrease In Filter Inductor And Capacitor	0.31%	2.43%
Verr (Max) For 20% Decrease In Filter Inductor	1.5v	22.10v
Verr (Max) For 20% Decrease In Filter Capacitor	1.7v	22.13v
Verr (Max) For 20% Decrease In Filter Inductor And Capacitor	1.8v	23.1v

The impact of improved (SMC) controller in the performance of multistage converter system is assist in terms of THD, Verror (max) and steady state error in power is shown in Table I and Table2 .These tables includes the results of the analysis of both the PI and SMC controller used with VSI for feeding nonlinear loads through a combination of PV source and supercapacitor.

5. Conclusion

An approach has been carried out in the paper which comprises of the integration of multistage converter system incorporating MPPT with boost converter, PI / SMC controllers with VSI for nonlinear loads, and an arrangement of PV source in combination with a supercapacitor feeds a non linear load separately. The analysis of performance of PV fed multistage converter system deploying SMC controlled VSI shows that under similar conditions both the THD as well as the output-voltage-error are less in comparison to those obtained with the conventional PI controlled VSI under identical loading conditions. Also it can be seen that with PI controller the output of VSI has very high steady state error between the power demand and supply. Thus the SMC Controlled VSI used with MPPT controlled PV generation can be a better option for integrating it to the micro grid systems. Further it was interesting to note that the controllers take due care of suitably integrating the supercapacitor to balance the intermittency of PV source.

References

- [1] Satish Kumar Gudey, Rajesh Gupta, "Second Order Sliding Mode Control for a Single Phase Voltage Source Inverter. IET Power Electronics 2014. <https://doi.org/10.1109/TENCON.2014.7022439>.
- [2] Abdel-Rahim, N.M., Quaicoe, J. E.: 'Analysis and design of a multiple feedback loop control strategy for single-phase voltage-source UPS inverters', IEEE Trans. Power Electron., 1996, 11, (4), pp. 532–541. <https://doi.org/10.1109/63.506118>.
- [3] Kawamura, A., Chuarayaratip, R., Haneyoshi, T.: 'Deadbeat control of PWM inverter with modified pulse patterns for uninterruptible power supply', IEEE Trans. Ind. Electron., 1988, 35, (2), pp. 295–300. <https://doi.org/10.1109/41.192662>.
- [4] Hua, C.: Two-level switching pattern deadbeat DSP controlled PWM inverter, IEEE Trans. Power Electron., 1995, 10, (3), pp. 310–317. <https://doi.org/10.1109/63.387996>.
- [5] Kukrer, O., Komurcugil, H.: 'Deadbeat control method for single-phase UPS inverters with compensation of computation delay', IEE Elect. Power Appl., 1999, 146, (1), pp. 123–128 <https://doi.org/10.1049/ip-epa:19990215>.
- [6] Ortega, R., Loria, A., Nicklasson, P.J., Sira-Ramirez, H.: 'Passivity-based control of Euler-Lagrange systems' (New York, Springer-Verlag, 1998). <https://doi.org/10.1007/978-1-4471-3603-3>.
- [7] Marquez, H.J.: 'Nonlinear control systems: analysis and design' (John Wiley & Sons, 2003).
- [8] W. Perruquetti and J.P.Barbot, Sliding Mode Control in Engineering, New York, Marcel Dekker; 2002. <https://doi.org/10.1201/9780203910856>.
- [9] J. J. E. Slotine and W. Li, Chapter 7, Sliding control, in Applied Nonlinear Control. Englewood Cliffs, NJ, Prentice-Hall, Inc., 1991.
- [10] V. Utkin, Sliding Modes in Control Optimization. Berlin: Springer-Verlag, 1992 <https://doi.org/10.1007/978-3-642-84379-2>.
- [11] S. Pandey, B. Dwivedi, A. Tripathi "Closed Loop Boost Converter Control of Induction Motor Drive fed by Solar Cells" ICETEES-ES, 11- 12 March 2016
- [12] Gudey, S.K., Gupta, R.: 'Sliding mode control in voltage source inverter based higher order circuits', Int. J. Electron., 2015, 102, (4), pp. 668–689. <https://doi.org/10.1080/00207217.2014.936523>.
- [13] Utkin, V.I.: 'Variable structure systems with sliding modes', IEEE Trans. Autom. Control, 1977, 22, (2), pp. 212–222. <https://doi.org/10.1109/TAC.1977.1101446>.
- [14] Hu, J., Shang, L., He, Y., Zhu, D.J.Q.: 'Direct active and reactive power regulation of grid-connected DC/AC converters using sliding mode control approach', IEEE Trans. Power Electron., 2011, 26, (1), pp. 210–222. <https://doi.org/10.1109/TPEL.2010.2057518>.
- [15] Pmheiro, H., Martins, A.S., Pinheiro, R.: 'A sliding mode controller in single phase voltage source inverters'. Proc. IEEE IECON, Bologna, September 1994, pp. 394–398.
- [16] Tai, T.L., Chen, J.S.: 'UPS inverter design using discrete-time sliding – mode control scheme', IEEE Trans. Power Electron., 2002, 18, (1), pp. 67–75.
- [17] Abrishamifar, A., Ahmad, A.A., Mohamadian, M.: 'Fixed switching frequency sliding mode control for single-phase unipolar inverters', IEEE Trans. Power Electron., 2012, 27, (5), pp. 2507–2514. <https://doi.org/10.1109/TPEL.2011.2175249>.
- [18] Suwat Sikkabut, et al Control strategy of solar/wind energy power plant with supercapacitor energy storage for smart DC microgrid, 2013 IEEE 10th International Conference on Power Electronics and Drive Systems (PEDS).
- [19] A. S.Weddell, G. V.Merrett, T. J. Kazmierski, and B. M. Al-Hashimi, "Accurate supercapacitor modeling for energy harvesting wireless sensor nodes," IEEE Trans. Circuits Syst. II, Exp. Brief, vol. 58, no. 12, pp. 911–915, Dec. 2011.
- [20] Zhongqiu Wang; Xi Li; Gengyin Li; Ming Zhou; K L Lo "Energy storage control for the Photovoltaic generation system in a micro-grid" 2010 5th International Conference on Critical Infrastructure (CRIS).